TU Delft

Delft University of Technology

Document Version
Final published version

Citation (APA)
Veldhuis, L., Stokkermans, T., Sinnige, T., & Eitelberg, G. (2016). Analysis of swirl recovery vanes for increased propulsive efficiency in tractor propeller aircraft. In *30th Congress of the International Council of the Aeronautical Sciences, ICAS 2016* International Council of the Aeronautical Sciences.

Important note
To cite this publication, please use the final published version (if applicable).
Please check the document version above.

Copyright
In case the licence states “Dutch Copyright Act (Article 25fa)”, this publication was made available Green Open Access via the TU Delft Institutional Repository pursuant to Dutch Copyright Act (Article 25fa, the Taverne amendment). This provision does not affect copyright ownership.
Unless copyright is transferred by contract or statute, it remains with the copyright holder.

Sharing and reuse
Other than for strictly personal use, it is not permitted to download, forward or distribute the text or part of it, without the consent of the author(s) and/or copyright holder(s), unless the work is under an open content license such as Creative Commons.

Takedown policy
Please contact us and provide details if you believe this document breaches copyrights.
We will remove access to the work immediately and investigate your claim.

This work is downloaded from Delft University of Technology.

ICAS 2016
30th Congress of the International Council of the Aeronautical Sciences
DCC, Daejeon, Korea ; September 25-30, 2016

ANALYSIS OF SWIRL RECOVERY VANES FOR INCREASED PROPULSIVE EFFICIENCY IN TRACTOR PROPELLER AIRCRAFT

Leo Veldhuis* , **Tom Stokkermans*** , **Tomas Sinnige*** , **Georg Eitelberg***
***Delft University of Technology**

Keywords: *Swirl recovcery, propellers, propulsive efficiency*

Abstract

In this paper we address a preliminary assessment of the performance effects of swirl recovery vanes (SRVs) in a installed and uninstalled tractor propeller arrangement. A numerical analysis was performed on a propeller and a propeller-wing configuration after the SRVs were optimized first in a separate process. The SRVs are essentially designed to recover the swirl in the rotor slipstream, thereby increasing the propulsive efficiency. To confirm the main flow effects of the SRVs, a separate windtunnel study was performed on a single-rotating propeller model in the large low-speed windtunnel. A steady RANS-based numerical analysis showed that the application of SRVs in a propeller-only model may lead to an increase of propulsive efficiency in the order of 2 %. In case of the SRVs in a representative tractor propeller-wing configuration, the positive effects are reduced due to the swirl recovery effect of the wing and the upwash effect in the SRV plane. The latter requires an optimization per SRV blade which was not performed in this particular study. In de experimental study performance data of the propeller were acquired with a rotating shaft balance. Furthermore, Particle Image Velocimetry PIV measurements in the slipstream of the propeller with and without SRVs substantiated the efficacy of the vanes in reducing the swirl in the propeller slipstream. Reductions of 50% in the swirl kinetic energy was observed at a medium thrust settings.

1 Introduction

Compared to modern turbofan engines propellers offer a significant reduction in aircraft fuel burn when the flight Mach number is not to high. The "open rotor" concept allows the bypass ratio to be increased to values unattainable by turbofans resulting in an increased the propulsive efficiency. However, this comes at the cost of a number of disadvantages compared to turbofans, thereby presenting challenges for the successful implementation of open rotor engines in next-generation aircraft. Even if the propeller may work at relatively high efficiency in cruise, losses due to swirl exist especially when a large number of blades is used and the propeller operates at higher loading conditions. Furthermore one major disadvantage of the open rotor system is its associated high level of noise emissions. The open rotor's most significant noise sources are those from the propeller blades, of which the emitted noise is not shielded by a casing as is the case for turbofans. By utilizing a second rotating blade row, contra-rotating propellers can recover the swirl energy, thereby increasing the propulsive efficiency in cruise by up to 8% [1, 2].

In all studies on contra-rotating propellers increased weight and complexity is expected compared to the application of modern single-rotations propeller. Hence, to further enhance the propulsive efficiency of propeller propulsion systems a research program on so-called swirl recovery vanes (SRV) was initiated at Delft Uni-

versity of Technology. In this case a stationary set of vanes (basically a stator) is used for which an efficiency gain is achieved with a system that is much simpler than contra-rotating open rotor (CROR) concept. Experimental studies by NASA, on a high speed propeller design confirmed the potential efficiency increase resulting from application of the SRVs, with measured efficiency gains of around 2 percent [3]. At the same time, numerical analyses based on solutions of the Euler equations predicted an efficiency increase of approximately 5 percent for the same configuration and operating conditions [4, 5]. Apart from the work performed by NASA and partners in the 1990s, more recently a CFD analysis using a RANS solver showed increased thrust levels due to application of the SRVs [6]. However, in the same study it was shown that the total system efficiency was reduced, stressing the importance of proper SRV design and integration.

Considering the limited number of studies devoted to SRVs published as of now, the effect of the SRVs on the aerodynamic and aeroacoustic performance of propeller propulsion systems is still largely unclear. Furthermore no studies have been performed to determine whether the SRV could acts as a means to further improve the propulsive efficiency of modern turboprop aircraft that fly at lower flight speeds than the projected ones for high speed open rotor designs. This study on SRVs aims at obtaining better understanding of the flow field associated with SRVs and its performance effects both from aerodynamic and acoustic perspective. To this purpose numerical studies have been initiated in which the SRV blade design has been optimized and analyzed using CFD based on a transient RANS analysis. Additionally an experimental campaign has been performed in which the swirl recovery capability and the noise production of the installed systems have been investigated. Some of the results obtained so far are summarized in the subsequent sections.

2 Preliminary analysis of swirl recovery effect

To get a basic understanding of the swirl recovery effect on the propulsive efficiency, a preliminary comparison can be made based on actuator disk theory (ADT), in which no swirl losses are present, and a blade element model (BEM). The latter is considered to provide quite acceptable performance data as long as the blades are not highly curved and compressibility effects can be neglected.

The propeller model that was used in this analysis is typical for a state of the art turboprop aircraft like the ATR-72 or the Fokker 50. The main parameters used in the analysis are presented in Table 1. The propulsive efficiency of the uninstalled propeller (i.e. propeller in axial flow without any interaction with the airframe) is defined by:

$$\eta = \frac{T V_\infty}{P} \tag{1}$$

where T is the thrust coefficient, V_∞ is the undisturbed flow speed, and P is the power input to the propeller.

As opposed to the ADT model, which only considers axial momentum, the BEM model incorporates both axial and swirl velocities as well as viscous losses. The latter is obtained by incorporating 2-dimensional lift and drag coefficient data that can be obtained either from viscous calculations on airfoils or from experiments. As such, a comparison between ADT and BEM performance data provides useful insight in the influence of viscous losses and swirl losses and

Table 1 Reference propeller data used in the Actuator Disk Theory model (ADT) and Blade Element model (BEM) comparison.

Parameter	Value
Number of blades, B	6
Diameter, D	$3.6\,m$
$\beta_{0.75R}$ @ cruise	$35.5\,deg$
$\beta_{0.75R}$ @ climb	$32.5 deg$
Airfoil	ARAD 13

Table 2 Effect of adaptations in the calculation model on the propulsive efficiency at different thrust coefficients for the reference propeller of Table 1. $T_c = 0.046$ is thrust coefficient at maximum efficiency in the BEM analysis, $T_C = 0.3$ is for cruise and $T_C = 0.56$ is for climb.

	$T_c = 0.046$, η_{ADT}=0.972		$T_c = 0.300$, η_{ADT}=0.859	
Adaptation	η_{BEM}	$\frac{\eta_{ADT}}{\eta_{BEM}}$	η_{BEM}	$\frac{\eta_{ADT}}{\eta_{BEM}}$
Original	0.884	1.100	0.742	1.158
No swirl	0.911	1.067	0.809	1.062

	$T_c = 0.560$, η_{ADT}=0.859	
Adaptation	η_{BEM}	$\frac{\eta_{ADT}}{\eta_{BEM}}$
Original	0.658	1.188
No swirl	0.721	1.085

it shows the maximum theoretical gain that can be obtained by swirl recovery, in any form. Table 2 presents the results for 3 thrust coefficients, T_c, for the uninstalled propeller (uniform inflow condition). In this case the thrust coefficient is defined as:

$$T_c = \frac{T}{\rho V_\infty^2 D^2} \tag{2}$$

When comparing the ADT data with that obtained from the original BEM analysis it is clear that a significant loss is introduced due to the generation of swirl. Depending on the loading condition the difference in the propeller efficiency is between 10% (low thrust, $T_c = 0.046$) and 18% (high thrust, $T_c = 0.56$). However, it should be noted that in the BEM case not only swirl but also tip losses and viscous losses are present. Therefore it it more appropriate to compare the efficiency for the original BEM case with that where swirl losses were neglected (i.e. maximum swirl recovery was obtained by combining the propeller with optimum SRV's). In that case we see that the efficiency increases with 3% for the low thrust case to 9.6% for the high thrust case. Apparently still quite a significant efficiency increase can be obtained by the application of SRV's although it should be emphasized that this analysis is based on the assumption that the swirl in the slipstream can by fully recovered. In practice this will be impossible due to the limited solidity of the SRV than can be applied. Last but not least the viscous losses due to the SRV's were neglected in this case.

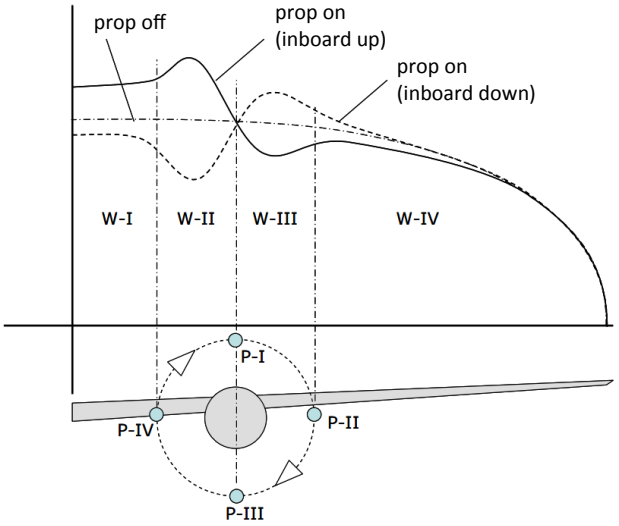

Fig. 1 Load distribution for different rotational direction of the propeller and influence areas on the wing (W-I to W-IV) and the propeller (P-I to P-IV) that are all affected by the interaction between propeller and wing [7]

As for most turboprop aircraft the propeller is often installed in a tractor fashion onto a wing, the application of SRV's will have an impact on the angle of attack as experienced by the part of wing that is washed by the propeller slipstream [7]. The resulting changes to the spanwise load distribution due to the swirl in the slipstream is dependent on the rotational direction of the propeller as qualitatively sketched in fig. 1.

As indicated by many researchers, the propeller induced flow field might actually reduce the overall lift induced drag, an effect that should be taking into account when SRV's are to be installed in a tractor propeller wing design. To get a further insight in the magnitude of these effects a combined numerical - experimental campaign was started performed. Some of the key outcomes will be discussed hereafter.

By combining a vortex-lattice model (VLM) for the wing and a BEM model for the propeller as discussed in [8] the influence of the swirl recovery on the overall propulsive efficiency of a

Table 3 Effect of swirl recovery by SRV's on a Fokker 50-like aircraft at cruise lift coefficient of $C_L = 0.3$ as determined by a simple combined VLM-BEM analysis. Advance ratio is held constant at J=1.058. Factor F_{v_t} is a multiplication factor by which the tangential velocity component, v_t, is decreased, to simulate the effect of swirl recovery.

F_{v_t}	$\Delta C_{D_i}(\%)$	$\Delta C_{D_p}(\%)$	$\Delta T_c(\%)$	$\Delta\eta(\%)$	$\Delta\eta_p$
0.75	7.6	0.4	10.8	1.4	0.009
0.50	11.2	1.2	19.6	2.3	0.016
0.25	12.1	2.2	26.9	3.1	0.021
0.00	12.8	3.2	33.1	3.6	0.024

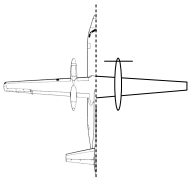

typical turboprop model was determined. An indication of the magnitude of a certain amount of swirl recovery (expressed through multiplying the swirl component in the slipstream by a reduction factor, F_{v_t}) is presented in table 3.

From this analysis, which was performed at a fixed advance ratio, a clear effect of the reduction in the swirl velocity component is evident. Reducing the value of v_t leads to a an increase in the induced drag. This phenomenon is in agreement with some earlier studies on propeller wing interaction. Also a small increase in the profile drag is recognizable as the flow speed is now more aligned with the undisturbed flow direction. Significant effects are found in the thrust coefficient as the swirl component contribution in the propeller induced flow field becomes smaller. Finally when analyzing the effect on the efficiency two definitions are considered. The first one is the propeller efficiency as defined in eq. 1. Again typical values of around 3-4% are found for full swirl recovery. An interesting definition of the overall propulsive efficiency, η_p, is given by:

$$\eta_p = \frac{-C_x' V_\infty}{P} \tag{3}$$

Here, C_x' is the effective axial force coefficient which is determined by the thrust and the drag of the propeller plus wing configuration. Under normal steady flight conditions, for the full aircraft, C_x will be zero (i.e. $T = D$). However, since the the drag of the wing is the only contribution that is accounted for, the propulsive efficiency, η_p, will have values larger than zero (i.e. $T > D$). Its value is an indication of the surplus of thrust power that is obtained when swirl recovery is applied. From the last column in table 3 we see that swirl recovery may have a very significant positive effect on the performance of the aircraft. The effective thrust power shows an increase up to 2.4% of the total power consumed. These values for the performance improvement due to SRV are in quite in agreement with that of other researchers [2, 3].

The analysis so far is based on rather simplified models of the propeller and the wing and as such will have limited predictive capability, Hence, to provide a more detailed understanding of the different phenomena that play a role, higher fidelity numerical analysis as well as a preliminary experimental assessment of SRV effects was performed.

3 Numerical study

To obtain detailed information on the aerodynamic interaction between the propeller, swirl recovery vanes and wing in a typical wing-mounted tractor arrangement in a cruise and a high-thrust condition, transient RANS CFD simulations were performed.

The propeller model used in this study is based on a 6-bladed propeller that was used during an experimental study within the APIAN-INF project (see section 4). In that project the acoustic and aerodynamic installation effects of a propeller installed in the wake field of a pylon as well as an uninstalled propeller combined with SRVs was investigated. Earlier wind tunnel test that were performed in the DNW-HST transonic wind tunnel provided blade pressure and slipstream measurements that were used for validation of the isolated propeller CFD model. Within

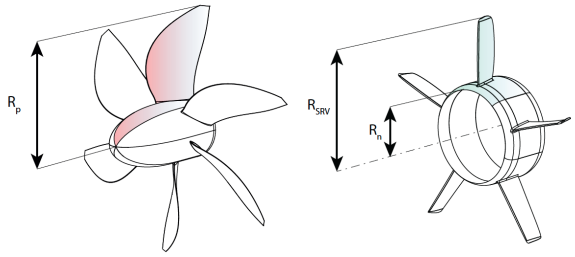

Fig. 2 APIAN propeller, spinner and hub with the blades set at $\beta_{0.75} = 40.4°$. The red part shows the wedge that was used in the CFD model of the uninstalled propeller (top) and SRV (bottom).

Table 4 Propeller characteristics of the APIAN propeller model.

Variable	Value
Scale	1:8
Propeller radius, R_p	250 mm
Propeller blade pitch $\beta_{0.75}$ at $0.75R_p$	40.4°
Propeller blade chord $c_{0.75}$ at $0.75R_p$	94.2 mm

the limitations of fully turbulent modeling of the boundary layer by means of scalable wall functions, good agreement is found with the experimental data, including the existence of a conical leading edge separation vortex at low advance ratios.

Fig. 2 shows an isometric view of the propeller and the SRVs while Table 4 summarizes the key propeller properties.

PIV measurements in a horizontal plane spanned by the radial direction and rotation axis provide a comparison of the slipstream velocity components and vorticity. Fig. 3 shows the measured and calculated tangential velocity component. As can be seen, a significant reduction of the swirl velocity, v_t, due to the presence of the SRVs is obtained. The CFD simulation combined with the PIV measurements enables an extensive description of the structure of root and tip vortices induced by the propeller blades and SRV as shown in Fig. 4.

A SRV analysis tool based on lifting-line the-

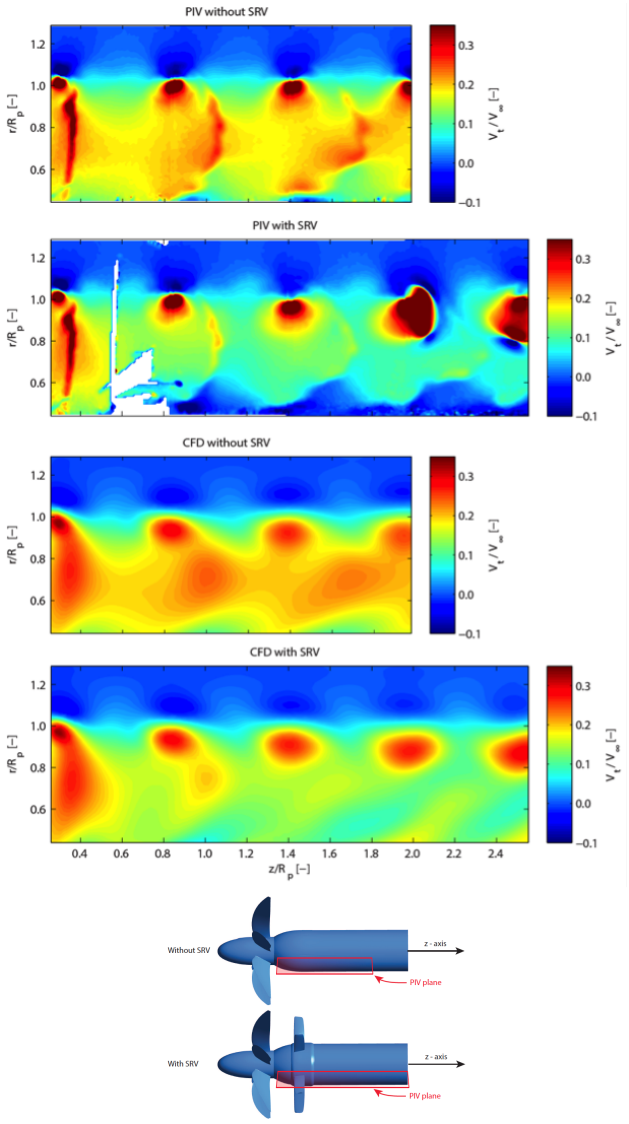

Fig. 3 Contour plots of the dimensionless tangential velocity measured by means of PIV in the APIAN-INF wind tunnel test compared to the results of transient RANS simulations with and without SRVs in a horizontal plane directly behind the propeller.

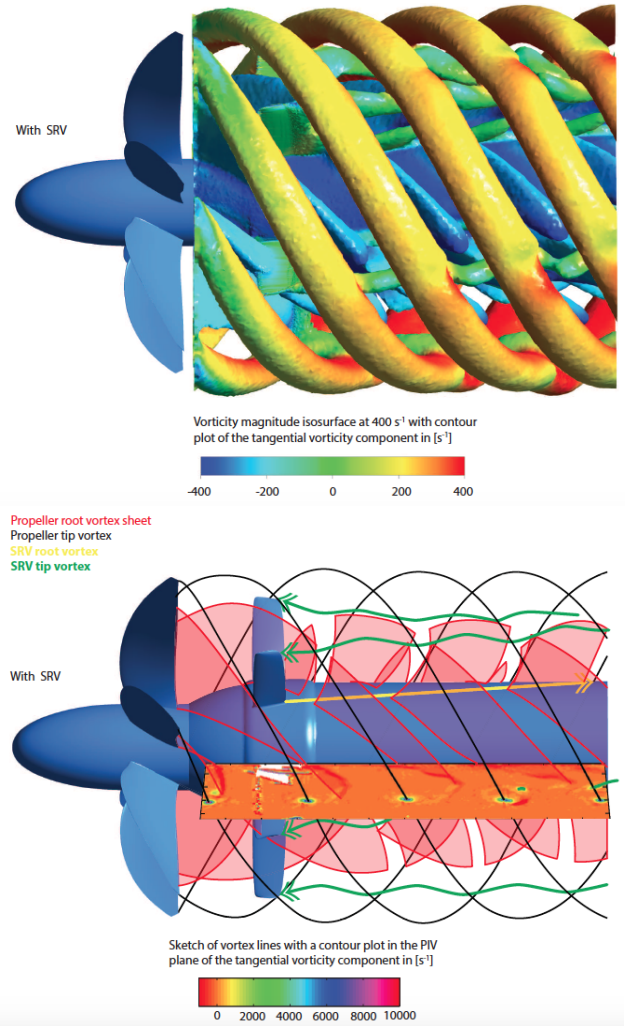

Fig. 4 Isosurface of calculated vorticity magnitude behind the APIAN propeller with SRVs installed including a contour plot of the tangential vorticity component (top) and sketch of the vortex lines with SRV including a contour plot of the tangential vorticity component measured by means of PIV (bottom).

ory modified for non-uniform inflow was developed which makes use of XFOIL, a design and analysis tool of subsonic isolated airfoils. In combination with an optimization routine, this tool allows for the design of swirl recovery vanes for an uninstalled configuration using the instantaneous velocity field from a propeller slipstream as inflow field [9]. From a simplified analysis of an elliptical vane in a flow with uniform swirl it is concluded that optimization for maximum SRV thrust is preferred over maximum swirl recovery to reach the highest gain in propulsive efficiency. Several design were investigated but the discussion in this paper is limited to design #1 which is optimized for the cruise condition with a constraint on stall for the high-thrust condition.

Uninstalled propeller-SRV simulations show that for the cruise phase (advance ratio $J = 1.60$) and for intermediate advance ratios between the cruise and high-thrust condition ($J = 0.95$), the propulsive efficiency benefit by the addition of swirl recovery vanes is very accurately estimated. Earlier onset of stall results in a deviation of propulsive efficiency benefit for the high-thrust condition. Residual swirl is left downstream of the SRV. Fig. 5 shows the estimated propulsive efficiency benefit and the radial distribution of circumferential averaged swirl angle in different planes in the slipstream without and with the SRV of design 1. The gain is typically between 0 and 3.5% depending on the propeller advance ratio.

Combining a trailing wing, based on the Fokker F-50 aircraft, with the APIAN propeller and SRV design 1, gives further insight in the total aircraft propulsive efficiency benefit. Two mechanism play a role here. Firstly, under normal circumstances the wing alone already recovers part of the swirl energy with a resulting affect on the local circulation in the slipstream washed area. As this phenomenon has an upstream effect it offsets the potential benefit of applying SRVs. Secondly, the slipstream tangential velocity component, that is affected by the SRVs, disturbs the original wing lift distribution which may result in an increased local wing induced drag (due to spanwise changes in the bound vorticity).

In case the resulting flow results in a reduced

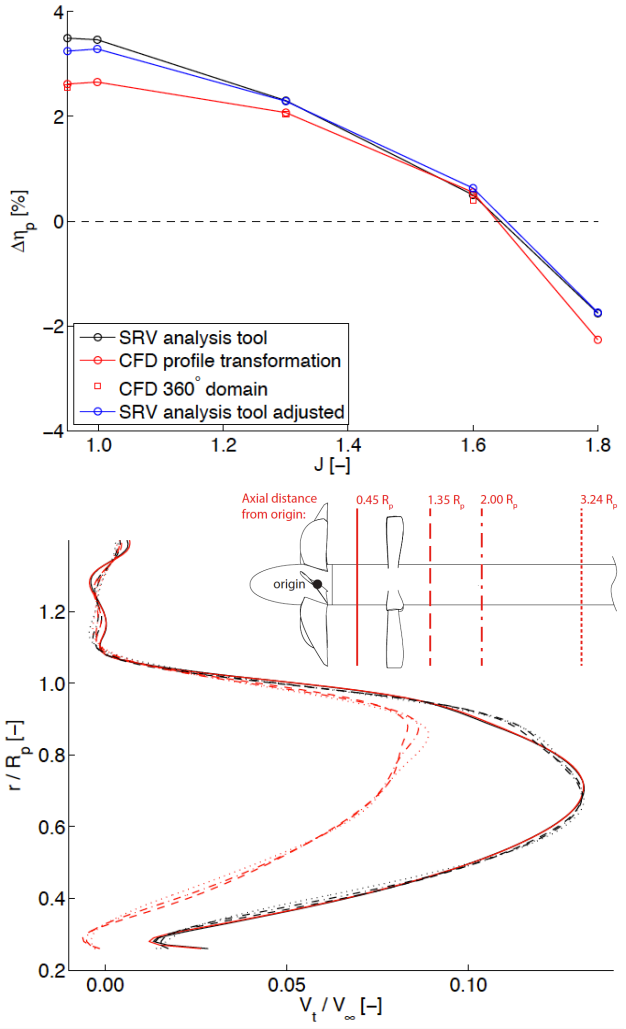

Fig. 5 Comparison of a conceptual SRV analysis tool and CFD showing an increase in propulsive efficiency by the addition of SRVs for various advance ratios J (top) and radial distribution of circumferential averaged swirl angle ϕ at different slipstream planes with and without SRV in the cruise condition (bottom).

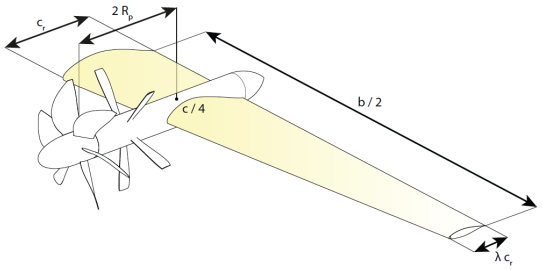

Layout of F50 like propeller wing model with SRV installed.

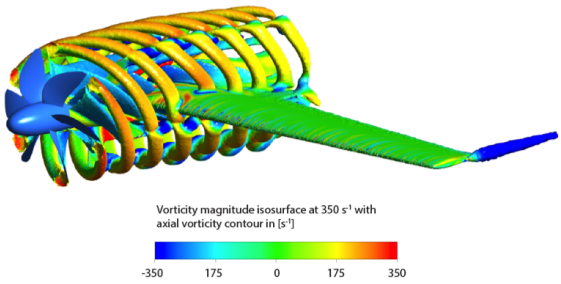

Fig. 6 Example of calculated isosurface of the vorticity magnitude behind the APIAN propeller with SRV and a Fokker 50 like half-wing colored by the level of the the axial vorticity component.

wing lift coefficient a larger wing angle of attack would be required when SRVs are present thus diminishing possible gains in performance. The trailing wing causes a disturbance of the structure of root and tip vortices from the propeller blades and swirl recovery vanes, which can be seen in fig. 6 showing an isosurface of the vorticity magnitude behind the propeller including a contour plot of the axial vorticity component.

Table 5 presents an overview of the forces acting on all relevant parts of the propeller wing configuration at advance ratios of $J = 1.6$ and $J = 1.3$. We see that at $J = 1.6$, with represents a rather low thrust coefficient, the addition of SRV results in a slight increase in propeller thrust, an increase in wing drag and a slight decrease in nacelle drag. Together with the net SRV thrust, the overall thrust is slightly lower than the one without SRV and thus it is better to have no SRV, from a thrust point of view. It should be noted that the SRV design used in this analysis is based on the assumption that the blades would face a axial symmetrical inflow. However, due to the strong upwash effect of the wing every

Table 5 Forces of all aerodynamic surfaces in thrust (T) and lift (L) direction for J=1.6 expressed in percentage of the values without SRV.

J=1.6				
Part	$T_{no\,SRV}$	T_{SRV}	$L_{no\,SRV}$	L_{SRV}
Propeller	100.00	100.24	0.85	0.86
SRV	-	0.88	-	0.05
Wing	-31.40	-32.69	100.00	100.20
Nacelle	-1.34	-1.22	6.30	6.41
Net	67.26	67.21	107.15	107.52
J=1.3				
Part	$T_{no\,SRV}$	T_{SRV}	$L_{no\,SRV}$	L_{SRV}
Propeller	100.00	100.12	0.98	0.99
SRV	-	3.32	-	-0.15
Wing	-12.64	-14.84	100.00	99.48
Nacelle	-0.98	-0.63	6.54	6.61
Net	85.38	87.97	107.52	106.93

blade of the vanes experience different inflow angles which deteriorates the beneficial effects on swirl recovery [9]. However, at $J = 1.3$ the net thrust is 1.84% higher due to the SRV because the propeller rotation starts to dominate the wing upwash effect even when the wing drag has increased.

The net increase in propulsive efficiency due to the addition of SRV can be defined as:

$$\Delta\eta_p = (\eta_p)_{with\,SRV} - (\eta_p)_{without\,SRV} \qquad (4)$$

Whereas for the uninstalled propeller the SRVs may enhance the propulsive efficiency by approximately 2% the installed configuration seems to lead to somewhat lower values. From the CFD calculations the resulting increase in propulsive efficiency, $\Delta\eta_p$, for $J = 1.6$ and $J = 1.3$ are -0.14% and +1.0%, respectively. These values are also considerably lower than the values found from the simplified VLM-BEM analysis as presented in table 3. The difference is to be attributed to the fact that in the simplified analysis a very efficient swirl recovery is assumed by the reduction of v_t over the complete 0-360 degree azimuthal range. With a finite number of

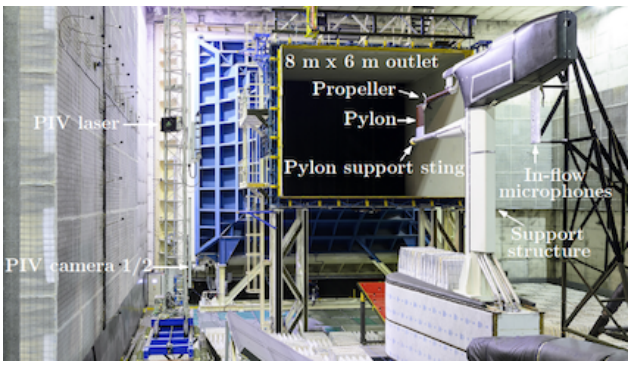

Fig. 7 Experimental setup, showing the propeller and swirl recovery vanes installed in the DNW LLF windtunnel.

SRV blades, as employed in the CFD analysis, this will never be attainable. Last but not least the SRV blades were not separately optimized for their local azimuthal position [9].

4 Experimental study

The effect of SRV installed behind the APIAN propeller was determined in a test campaign in the large low-speed facility (LLF) of the German-Dutch wind tunnels (DNW). The dimensions of the test hall are around 50 m x 30 m x 20m, while an open jet configuration was selected with 8 m x 6 m outlet. An image of the test setup is shown in fig. 7.

The six-bladed propeller model with a diameter of 0.508 m was originally developed for the European APIAN (Advanced Propulsion Integration Aerodynamics and Noise) project [10, 11]. The blade angle was set to a fixed value of 40.4 degrees at 75% of the radius. A design rotor advance ratio of $J = 1.75$ was selected, based on the requirement for the system to offer good performance in cruise conditions. To reduce interaction noise a total of 5 vanes was chosen, while the diameter of the SRVs was cropped to 90% of that of the propeller to prevent additional noise due to blade-vortex interactions. Furthermore, a NACA 0009 cross-section was selected for the entire vane as it offered the best performance in terms of the predicted system efficiency gain of the airfoils considered in the optimization process [12]. The spacing between the front rotor

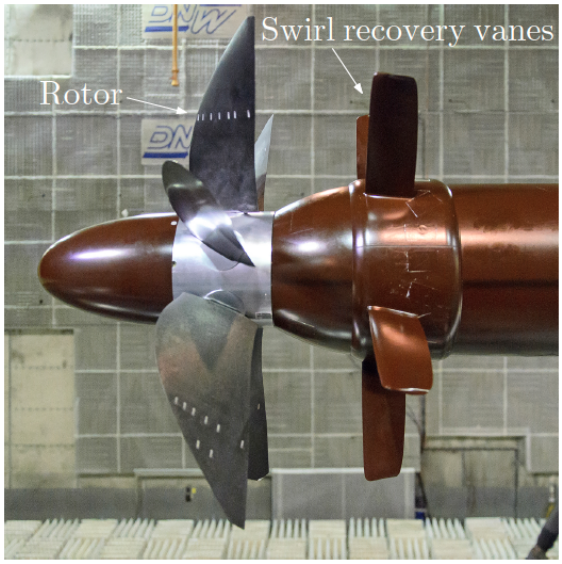

Fig. 8 APIAN propeller model in the DNW-LLF windtunnel with swirl recovery vanes installed.

and the SRVs was equal to approximately 30% of the propeller diameter (fig. 8).

During all measurements the propulsive performance of the propeller model was monitored using a Rotating Shaft balance (RSB). The SRVs were not instrumented, hence no information was available of their contribution to the total system thrust and efficiency. The forces and moments generated by the propeller were expressed in the form of a thrust coefficient C_T , torque coefficient C_Q, and propeller efficiency η.

The propeller propulsive performance is presented in fig. 9. Estimations of the variation of repeated measurements were made by considering the multiple data points obtained at the three advance ratios considered for the largest part of the test program and are indicated by the error bars. At an advance ratio of $J = 1.05$ a variation of 1% of the measured thrust coefficient was found, whereas at the lower thrust setting corresponding to $J = 1.75$ the variation of the acquired thrust coefficient equaled 5%.

Fig. 9 shows that the upstream effect of the SRVs on the performance of the propeller is negligible. For all advance ratios the change in performance remains within the statistical uncertainty of the measurements, with a difference of at most 1% compared to the performance of the

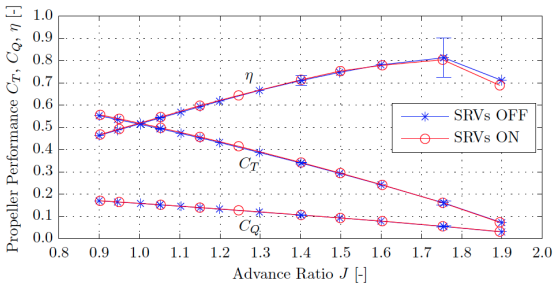

Fig. 9 SRV installation effect on the APIAN propeller performance.

isolated propeller. This is as expected considering the relatively small ratio of the loads generated by the vanes relative to the rotor.

To visualize the aerodynamic effects of the SRVs on the propeller slipstream, the flow downstream of the propeller with and without swirl recovery vanes was evaluated using PIV. Fig. 10 presents an example of the slipstream flow field behind the isolated propeller, at all eleven phase angles considered. Vorticity isosurfaces are plotted together with contours of the difference between the local and free-stream axial velocity components. As can be seen a high data fidelity was obtained from the PIV measurements.

Based on these PIV data it was possible to quantify the amount of swirl present in the propeller slipstream. For this purpose a swirl kinetic energy ratio, ε_k, is defined:

$$\varepsilon_k = \frac{E_k^{swirl}}{E_k^{\infty}} = \frac{V^2 + W^2}{U_{\infty}^2} \tag{5}$$

where U, V, and W are the streamwise, lateral, and vertical velocity components, respectively.

Fig.11 confirms the decrease in swirl kinetic energy in the propeller slipstream due to installation of the SRVs. Downstream of the vanes (fig.11, bottom) a reduction of up to 95% is achieved in the most inboard part of the slipstream. With increasing radial coordinate the amount of swirl recovery decreases linearly to zero around the blade tip. Integrated over the entire radial domain considered, the presence of the SRVs reduces the swirl kinetic energy by approximately 50%.

Upstream of the SRVs (fig.11, top) the swirl

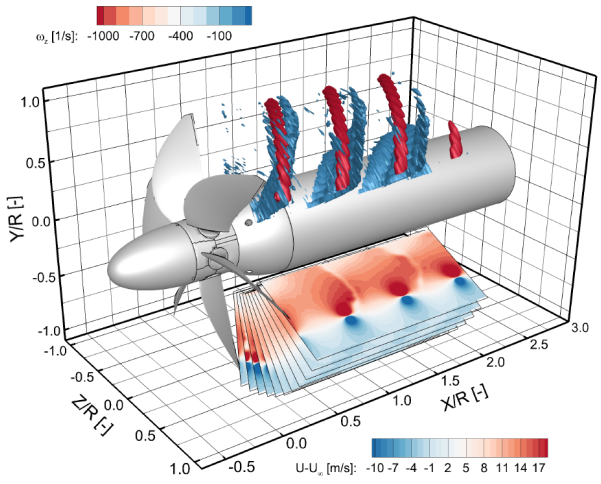

Fig. 10 Contours of streamwise velocity component with free-stream value subtracted (bottom part) and vorticity isosurfaces (top part) measured for the isolated propeller at $J = 1.40$.

is increased which is the result of the upwash generated by the lifting vanes. Note that the installation of the SRVs removes the axissymmetry of the flow field, hence the single PIV plane does no longer provide an integral view of the entire slipstream as for the isolated propeller case. Although the SRVs clearly remove a considerable part of the swirl, which is expected to lead to an increased efficiency, values on the net efficiency improvement could not be obtained as no separate SRV force balance was available. Hence, an experimental validation of the theoretical CFD-based results will be performed in an upcoming experiment at Delft University.

5 Conclusions

From the numerical and the experimental analysis of the propeller with installed swirl recovery vanes the following main conclusions may be drawn:

- From an numerical analysis on an uninstalled and an installed propeller (tractor configuration) with and without SRVs is was found that an optimized vane design may lead to an increase in propulsive efficiency of approximately 2%.

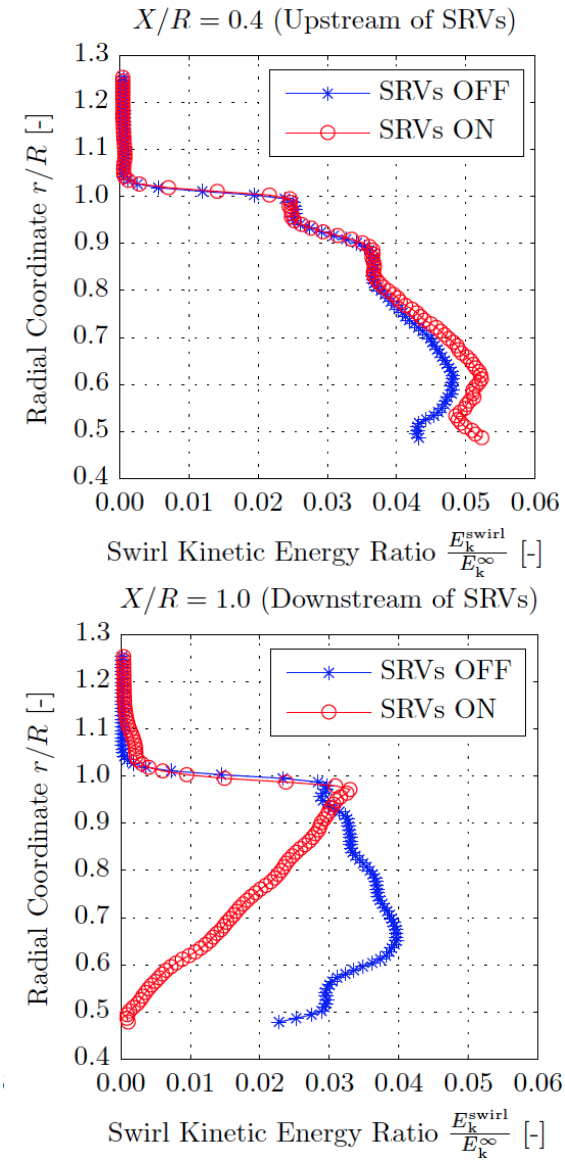

Fig. 11 Swirl kinetic energy ratio profiles with and without swirl recovery vanes, installed at streamwise positions upstream (top) and downstream (bottom) of the vanes; $J = 1.40$.

- In case of the propeller wing configuration a considerable amount of swirl is already recovered by the wing and the SRVs seems to have limited effect when their blade optimization does not take the wing induced upwash into account. Maximum values found for the overall efficiency increase found from the CFD calculation are around 1%.
- The experimental study showed that the installation of the SRVs led to very small changes in the integral propeller performance parameters over the complete advance ratio range considered. Hence, it is concluded that the upstream effect of the swirl recovery vanes on the time-averaged propeller performance is negligible in the current propeller-SRV layout.
- The SRVs indeed resulted in a swirl recovery and at the same time a small increase in axial flow speed (not shown herein). This provides further proof that the SRVs enhance the propulsive efficiency.
- At a medium thrust condition the integrated reduction in swirl kinetic energy equaled 50%, with the largest reductions obtained at the inboard radial stations.

References

[1] Strack, W. C., Knip, G., Weisbrich, A. L., Godston, J., and Bradley, E., Technology and Benefits of Aircraft Counter Rotation Propellers, NASA-TM-82983, 1982

[2] Mikkelson, D.C., Mitchell, G.A., Bober, L.J., Summary of recent NASA Propeller Research, NASA Technical Memorandum 83733, 1984

[3] Gazzaniga, J. and Rose, G., Wind tunnel performance results of swirl recovery vanes as tested with an advanced high speed propeller, 28th Joint Propulsion Conference & Exhibit, 1992, Nashville, TN, USA

[4] Miller, C. J., Euler Analysis of a Swirl Recovery Vane Design for Use With an Advanced Single-Rotation Propfan, 24th Joint Propulsion Conference & Exhibit, 1988, Boston, MA, USA

[5] Yamamoto, O., Numerical Calculation of Propfan/Swirl Recovery Vane Flow Field, 28th Joint Propulsion Conference & Exhibit, 1992, Nashville, TN, USA.

[6] Yangang, W., Qingxi, L., Eitelberg, G., Veldhuis, L.L.M., and Kotsonis, M., Design and numerical investigation of swirl recovery vanes for the Fokker 29 propeller, Chinese Journal of Aeronautics, Vol. 27, No. 5, 2014, pp. 1128-1136.

[7] Veldhuis, L.L.M., Propeller Wing Aerodynamic Interference, PhD dissertation, Delft University of Technology, 2005.

[8] Veldhuis, L.L.M., Review of propeller-wing aerodynamic interference, ICAS 2004-6.3.1, 2004

[9] Stokkermans, T.C.A., Design and Analysis of Swirl Recovery Vanes for an Isolated and a Wing Mounted Tractor Propeller, MSc Thesis, Delft University of Technology, 2015.

[10] Custers, L.G.M. and Elsenaar, A., Test report of the APIAN wind tunnel test in the DNW-HST. Technical Report NLR-CR-98571, Nationaal Lucht- en Ruimtevaartlaboratorium, 1999.

[11] Beaumier, P., Numerical Tools Developed at ONERA for the Aerodynamic Assessment of Propellers and Counter-Rotating Open Rotors, ICAS 2012-4.7.1, 2012.

[12] Kuijk, J.J.A. van, Analysis of Swirl Recovery Vanes - Propulsion system performance and slipstream-wing interaction, MSc Thesis, Delft University of Technology, 2015.

Copyright Statement

The authors confirm that they, and/or their company or organization, hold copyright on all of the original material included in this paper. The authors also confirm that they have obtained permission, from the copyright holder of any third party material included in this paper, to publish it as part of their paper. The authors confirm that they give permission, or have obtained permission from the copyright holder of this paper, for the publication and distribution of this paper as part of the ICAS proceedings or as individual off-prints from the proceedings.